Support information
Co-agglomerated Crystals of CL-20 with Insensitive Nitrogen-rich Energetic Materials

Junmao Hong [a,1], Jinchao Ma [a,*,1], Xinwei Huang [a], Kunyou Shi [a], Fang Li [a], Chuan Xiao [b], Hua Qian [a,*]

[a] School of Chemistry and Chemical Engineering, Nanjing University of Science and Technology, Nanjing 210094, P.R. China

[b] China North Industries Corporation, Beijing 100000, P.R. China

[*] Corresponding authors.

Email address: mjinchao@njust.edu.cn (J. Ma); qianhua@njust.edu.cn (H. Qian).

[1] These authors contributed equally.

MENU

S1 Materials and methods

S1.1 Materials

ε-2,4,6,8,10,12-hexanitro-2,4,6,8,10,12-hexaazaisowurtzitane (ε-CL-20) was provided by Qingyang Chemical Co., Ltd. α-CL-20 was prepared by a solvent/anti-solvent (acetone/water) method according to literature.[1]

To prepare CL-20-based CACs, bis([1,2,4]triazolo)[1,5-b:5',1'-f][1,2,4,5]tetrazine-2,7-diamine (DATC), 4,4'-(triaz-1-ene-1,3-diyl)bis(1,2,5-oxadiazol-3-amine) (DATF) and N^5,$N^{5'}$-(1,2,4,5-tetrazine-3,6-diyl)-bis(1*H*-1,2,4-triazole-3,5-diamine) (BTAAT) were respectively adopted as nitrogen-rich energetic materials (NEMs).[2-5]

Dimethyl sulfoxide (DMSO), ethanol (EtOH) and ethyl acetate (EA) were produced by General-reagent. Trichloromethane (TCM) was produced by Sinopharm Chemical Reagent Co., Ltd. All reagents were analytic reagent.

S1.2 Preparation of co-agglomerated crystals (CACs)

General preparation process of CAC has been described in texts. The detailed information on the preparation of CACs, co-precipitates and physical mixtures were listed in Table S1.

As a typical preparation process of CACs, 4 g CL-20 and 1 g NEMs were blended in an adequate amount of DMSO under proper temperatures (for CL-20/DATC system: 68 mL, 90℃; for CL-20/DATF system: 30mL, room temperature; for CL-20/BTAAT system: 80 mL, 90℃). The systems were then quick poured into

water with a volume of 15 to 20 times that of DMSO. The formed suspension was stirred to sufficiently precipitate CL-20 and NEM. The obtained co-precipitates were then gently boiled in TCM (6 mL per gram of co-precipitate) for 4 hours. Finally, the systems were cooled and the CACs were obtained by filtration and drying.

Physical mixtures were prepared in the actual ratios of CL-20 and NEMs in obtained CACs by manual wet grinding in an agate mortar with EtOH (for CL-20/DATC and CL-20/BTAAT systems) or water (for CL-20/DATF system) for 15 minutes.

Table S1 The preparation detail of CACs

Sample Code[a]	Co-formers[b]	Blending method[c]	Blending solvent system	Co-agglomeration?[d]
1-CP	CL-20/DATC	SAS	DMSO/water	No
1-CAC	CL-20/DATC	SAS	DMSO/water	Yes
1-PM	CL-20/DATC	PM	EtOH	No
2-CP	CL-20/DATF	SAS	DMSO/water	No
2-CAC	CL-20/DATF	SAS	DMSO/water	Yes
2-PM	CL-20/DATF	PM	water	No
3-CP	CL-20/BTAAT	SAS	DMSO/water	No
3-CAC	CL-20/BTAAT	SAS	DMSO/water	Yes
3-PM	CL-20/BTAAT	PM	EtOH	No

[a]Coding rules: The number before the short dash is the numerical order of different co-formers. The number after the short dash is the code for co-precipitate obtained by quickly solvent/anti-solvent methods without agglomeration process (CP), co-agglomerated crystal (CAC) or physical mixture (PM).

[b]The feed mass ratio of CL-20/NEMs was 4:1, i.e., 4 mass equiv CL-20 was used with 1 mass equiv NEMs.

[c]Code for blending method: SAS – solvent/anti-solvent method. Solutions of CL-20 and NEMs were quickly poured into anti-solvent to form co-precipitate; PM – physical mixing method. CL-20 and NEMs were put into an agate mortar and blended by manually grinding.

[d]Yes – Materials experienced an agglomeration process, i.e., were boiled in chloroform; No – Materials did not experience an agglomeration process.

S1.3 Characterization method

The component proportions of CL-20 and NEMs in CACs were determined by HPLC using external standard method. The morphology of materials was investigated using scanning electron microscope (SEM, ZEISS Sigma 300). Powder X-ray diffraction (PXRD) data were recorded at room temperature by Bruker D8 Discover powder diffractometer. Fourier Transform Infrared (FTIR) spectra were obtain using Thermo NICOLETIS20 spectrometer under ATR mode.

The ratios of CL-20 and NEMs in CACs were determined using a solvent extraction method: firstly, about 0.5 g sample was precisely weighed by difference and placed into a filter cup of known mass; then an excess of anappropriate saturated solution (for CL-20/DATC and CL-20/BTAAT: NEM-saturated EA solutions; for CL-20/DATF: CL-20-saturated EtOH solution) was used to wash the sample under stirring; finally, the filter cup was dried and weighed. The mass fraction was

calculated by Eq.(S1) and converted to molar ratio.

$$\omega_X = \frac{m_1 - m_2}{m_S} \quad \text{(S1)}$$

where ω_X is the mass fraction of component X in CACs (for CL-20/DATC and CL-20/BTAAT, X is CL-20; for CL-20/DATF, X is DATF); m_1 is the total mass of filter cup and samples before washing, g; m_2 is the total mass of filter cup and residua after washing, g; m_S is the mass of samples weighed by difference.

Densities of CACs and PMs were measured by gas pycnometer AccuPyc II 1345 at 30°C, using Helium as the analysis gas.

S1.4 Performance evaluation

Mechanical Sensitivities (impact and friction) were respectively determined by HWP18-30S BAM impact sensitivity tester and HWP17-10S BAM friction sensitivity tester (Hangzhou Young Instrument Science & Technology Co., Ltd.), using critical impact energy and critical friction load pressure as evaluation indexes, according to the section 13.4.2 and 13.5.1 of the UN Manual of Tests and Criteria (ST/SG/AC.10/11/Rev.7).[6] Mechanical sensitivity tests were conducted with a sample amount of 40 mm^3 for impact sensitivity and 10 mm^3 for friction sensitivity.

Thermal analysis was conducted by differential scanning calorimeter (Nanjing Dazhan Testing Instrument, DZ-DSC300) in 50 mL/min N_2 flow. A sealed stainless-steel crucible was used. Tests were conducted under heating rates of 5, 10, 15 and 20 K/min.

Detonation performance (detonation velocity and detonation pressure) was calculated using Kamlet equations (Eqs.(S2~S4)).

$$P = 1.588\rho_0^2\varphi \quad \text{(S2)}$$

$$D = 1.01\varphi^{0.5}(1 + 1.3\rho_0) \quad \text{(S3)}$$

$$\varphi = 0.489N\bar{M}^{0.5}Q^{0.5} \quad \text{(S4)}$$

where P is detonation pressure, GPa; ρ_0 is density, g/cm^3; φ is the characteristic value of explosive; D is detonation velocity, km/s; N is the number of moles of gaseous explosion products per gram of explosive, mol; $\bar{M}$ is the average molar mass of aseous explosion products; Q is the constant-volume heat of explosion of explosive, J/g, calculated by Hess' law.

S2 XRD analysis

For ε-CL-20, main diffraction peaks are at 10.70°, 12.60°, 12.80°,13.85°, 15.80°, 16.30°, 17.70°, 20.00°, 21.55°, 22.00°, 22.30°, 22.65°, 23.65°, 24.25°, 25.80°, 27.85°, 28.40°, 28.75°, 29.60°, 29.95° and 30.35°.

For α-CL-20, main diffraction peaks are at 12.21°, 13.85°,15.10°, 17.63°, 18.10°, 19.04°, 20.28°, 25.13°, 27.69°, 28.13° and 28.99°.

For 1-CAC, main diffraction peaks are at 12.19°, 13.81°, 15.10°, 17.61°, 18.12°, 19.03°, 20.28°, 25.09°, 27.72°, 28.10° and 28.97°.

For 1-PM, main diffraction peaks are at 10.79°, 12.66°, 12.91°, 13.91°, 15.12°, 15.82°, 16.42°, 17.84°, 20.10°, 21.94°, 22.09°, 22.33°, 22.74°, 24.35°, 25.09°, 25.91°, 27.98°, 28.52°, 28.86°, 29.71°, 30.06° and 30.47°.

For DATC, main diffraction peaks are at 15.01°, 24.81° and 29.37°.

For 2-CAC, main diffraction peaks are at 12.13°, 13.45°, 13.78°, 13.96°, 15.04°, 16.57°, 17.57°, 18.04°, 19.01°, 20.24°, 25.06°, 27.00°, 27.67°, 28.04°, 28.44° and 28.93°.

For 2-PM, main diffraction peaks are at 10.80°, 12.70°, 12.94°, 13.92°, 14.14°, 15.86°, 16.47°, 16.63°, 16.73°, 17.84°, 20.07°, 22.11°, 22.42°, 25.92°, 28.00°, 28.50°, 28.55°, 28.85°, 30.09° and 30.44°.

For DATF, main diffraction peaks are at 16.13°, 16.73°, 18.23°, 20.34°, 23.48°, 25.95°, 26.98°, 28.45°, 29.03°, 29.46° and 30.88°.

For 3-CAC, main diffraction peaks are at 12.17°, 13.82°, 13.98°, 17.61°, 18.08°, 20.28°, 22.35°, 25.12°, 27.71°, 28.08°, 28.95° and 29.34°.

For 3-PM, main diffraction peaks are at 10.85°, 12.74°, 12.90°, 13.98°, 15.88°, 16.43°, 17.18°, 17.81°, 21.70°, 22.09°, 22.42°, 22.75°, 23.80°, 24.39°, 25.27°, 25.98°, 28.02°, 28.54°, 28.87°, 29.34°, 30.11° and 30.48°.

For BTAAT, main diffraction peaks are at 12.68°, 17.14°, 20.67°, 22.40°, 25.23°, 28.27° and 29.28°.

S3 FTIR analysis

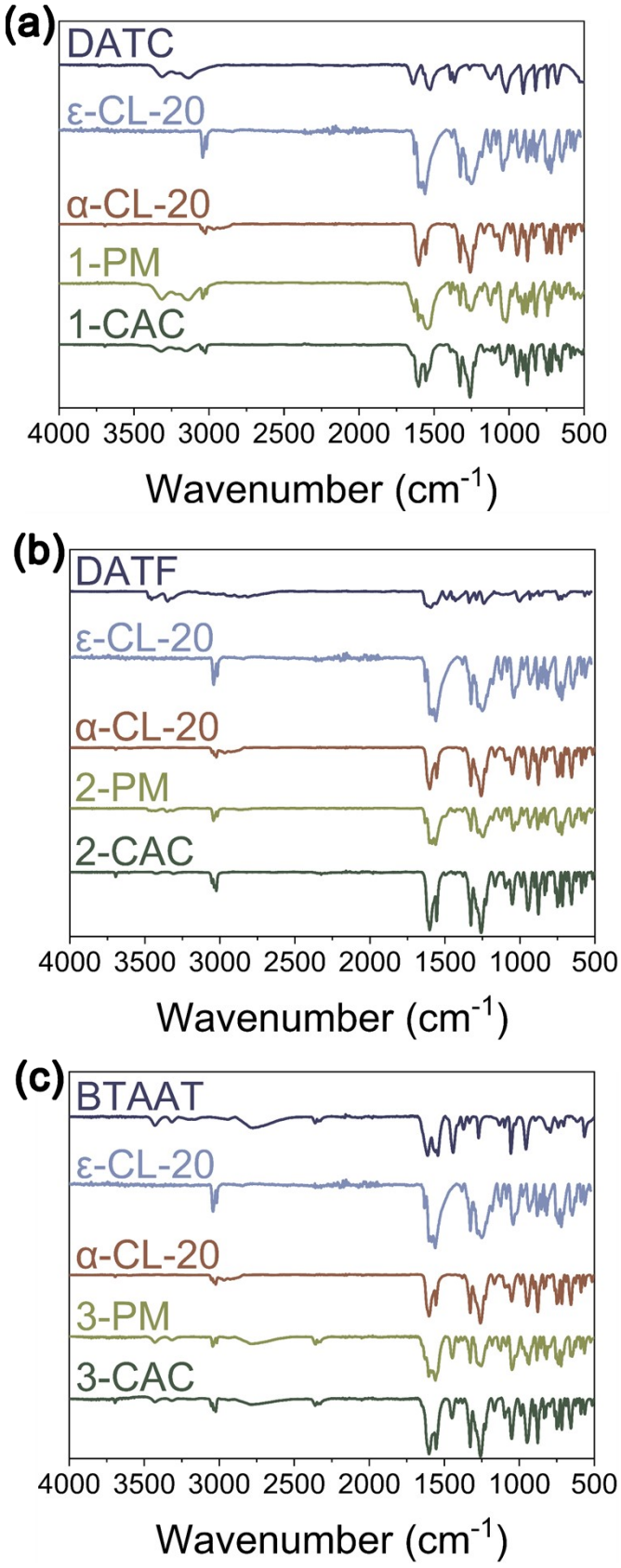

Fig. S1 The FTIR spectra of CACs, PMs and raw materials ((a) CL-20/DATC; (b) CL-20/DATF; (c) CL-20/BTAAT)

Table S2 Main absorption peaks and corresponding assignment of co-formers and CACs

Assignment[a]	ε-CL-20	α-CL-20	DATC	1-CAC	1-PM
$\nu_{N\text{-}H}$ for amino group			3312, 3213, 3140	3319, 3217, 3155	3313, 3209, 3137
$\nu_{C\text{-}H}$	3042, 3017	3053, 3037, 3024, 2968		3053, 3036, 3024	3042, 3016
$\delta_{N\text{-}H}$			1637, 1526		1632
$\nu_{C\text{-}N}$ for amine	1631, 757	750, 741	1390, 1364, 1264	740	1390, 1363, 743
ν_{as} for nitro groups	1602, 1584, 1560	1603, 1556		1602, 1554	1603, 1584, 1541
ν_{s} for nitro groups	1382, 1278, 1250	1381, 1259, 1228		1390, 1259, 1228	1389, 1280, 1252
$\nu_{C\text{-}N}$ for nitro groups	1326	1327		1327	1326
ν_{ring}	1181, 1135, 1123, 1086, 1039, 934, 882, 854, 830, 818, 737, 720, 646, 623, 589, 565	1167, 1095, 1078, 1051, 989, 947, 902, 877, 835, 825, 715, 688, 656, 625, 607 588, 563, 515	1124, 1018, 905, 824, 743, 678, 502	1165, 1124, 1095, 1045, 989, 947, 904, 877, 823, 717, 685, 656, 625, 588, 563	1181, 1133, 1123, 1090, 1018, 935, 907, 881, 854, 819, 721, 682, 658, 647, 623, 604, 589, 581, 565, 525

[a] ν – stretching vibration; ν_{as} – asymmetrical stretching vibration; ν_{s} – symmetrical stretching vibration; δ – bending vibration.

Table S2 (continue) Main absorption peaks and corresponding assignment of co-formers and CACs

Assignment[a]	DATF	2-CAC	2-PM	BTAAT	3-CAC	3-PM
$\nu_{N\text{-}H}$ for amino group	3456, 3349	3426, 3308	3458, 3352	3429, 3317	3430, 3315	3430, 3315
$\nu_{C\text{-}H}$		3053, 3038, 3024	3043 3016		3053, 3037, 3024	3042, 3017
$\delta_{N\text{-}H}$	1592, 1557			1610, 1543		1559
$\nu_{C\text{-}N}$ for amine	1338, 1291, 1240	739	1632	1442, 1372, 1334, 1272	1448, 1408, 1379, 740	1445, 1407, 757, 750, 743
ν_{as} for nitro groups		1602, 1555	1603, 1585, 1562		1602, 1556	1604
ν_{s} for nitro groups		1380, 1258, 1228	1383, 1281, 1248		1259, 1228	1380, 1253
$\nu_{C\text{-}N}$ for nitro groups		1327	1327		1327	1327
ν_{ring}	1127, 1002, 933, 911, 870, 853, 740, 721, 694, 568, 540	1166, 1095, 1080, 1051, 989, 946, 904, 877, 835, 716, 688, 656, 625, 608, 589, 563, 515	1182, 1136, 1124, 1088, 1043, 1018, 978, 935, 881, 854, 829, 818, 739, 721, 658, 648, 623, 588, 565, 524	1132, 1098, 1057, 956, 894, 794, 741, 704, 613, 566	1166, 1124, 1096, 1051, 989, 948, 902, 877, 835, 823, 794, 715, 688, 656, 625, 607, 588, 563, 515	1181, 1135, 1124, 1088, 1049, 935, 882, 854, 830, 819, 738, 721, 705, 659, 647, 624, 605, 589, 581, 566, 526

Table S3 The actual peak intensities for amino

Sample	Wavenumber of peak for amino (P_A) [cm^{-1}]	Transmittance for P_A (T_A) [%]	Transmittance for baseline at P_A (T_B) [%]	Actual peak intensity T_B-T_A [%]
DATC	3312.142	87.86835	100.01698	12.14863
	3136.652	86.65924	99.98302	13.32378
1-CAC	3319.044	93.19613	100.02296	6.82683
	3155.117	93.51346	100.04244	6.52898
1-PM	3313.106	83.21028	98.72666	15.51638
	3140.509	82.47234	99.43973	16.96739
DATF	3456.295	91.58237	100.09423	8.51186
	3348.783	89.73016	100.05263	10.32247
2-CAC	3426.079	96.25752	97.85371	1.59619
	3308.437	96.11901	97.82965	1.71064
2-PM	3457.900	97.06784	99.91935	2.85151
	3351.829	96.43481	100	3.56519
BTAAT	3428.971	91.05320	100.10187	9.04867
	3317.115	94.59167	99.88398	5.29231
3-CAC	3429.936	96.59734	101.42615	4.82881
	3315.187	97.93417	100.38625	2.45208
3-PM	3429.936	94.23798	100.15280	5.91482
	3315.187	96.65571	99.86418	3.20847

S4 Thermal analysis

S4.1 Methods

Thermal analysis of CACs and corresponding raw materials was performed from 50 to 500 ℃ by Differential Scanning Calorimetry (DSC, Nanjing Dazhan Testing Instrument, DZ-DSC300) at the heating rates of 5, 10, 15 and 20 K/min. Closed stainless steel crucibles were used. Sample loading mass was determined according to their thermal effect level (≤0.2 mg for pure CL-20; about 0.3 mg for DATF, CACs and PMs; 0.5~0.6 mg for DATC and BTAAT). The kinetics and thermodynamics of decomposition were analyzed.

(1) Kinetics

The peak temperatures of CACs, PMs and raw materials when the heating rate is zero were calculated by Eq.(S2) [7].

$$T_{pi} = T_{p0} + b\beta_i + c\beta_i^2 + d\beta_i^3 \tag{S2}$$

where T_{pi} is peak temperature under heating rate β_i, K; T_{p0} is peak temperatures when the heating rate is zero, K; β_i is heating rate, K/min.

The activation energy of CACs, PMs and raw materials was calculated using Kissinger method (Eq.(S3)) and Ozawa method (Eq.(S4)) method respectively [8, 9].

$$\ln\frac{\beta_i}{T_{pi}^2} = \ln\frac{A_K R}{E_{aK}} - \frac{E_{aK}}{RT_{pi}} \tag{S3}$$

$$\lg\beta_i = \lg\frac{A_O E_{aO}}{R f_O(\alpha)} - 2.315 - 0.4567\frac{E_{aO}}{RT_{pi}} \tag{S4}$$

where β_i is heating rate, K/min; T_{pi} is peak temperature under heating rate β_i, K; A is pre-exponential factor; R is the ideal gas constant, 8.314 J/(mol·K); E_a is activation energy, J/mol; α is conversion rate; $f(\alpha)$ is the function versus conversion rate reflecting reaction mechanism.

The critical temperatures of thermal explosion of CACs, PMs and raw materials were calculated by Eq.(S5) [10].

$$T_b = \frac{E_a - \sqrt{E_a^2 - 4E_a R T_{p0}}}{2R} \tag{S5}$$

where T_b is critical temperatures of thermal explosion, K; E_a is the average activation energies calculated by Kissinger method and Ozawa method, J/mol.

Moreover, Friedman (Eq.(S6)) and combined kinetic analysis (CKA) (Eq.(S7)) methods was utilized to further analyze the progress and mechanism of thermal decomposition.[11-13]

$$\ln\left[\beta\frac{d\alpha}{d\left(T - T_0\right)}\right] = \ln\left[A_F f_F(\alpha)\right] - \frac{E_{aF}}{RT} \tag{S6}$$

$$\frac{d\alpha}{d\left(T - T_0\right)} = \frac{A_{CKA}}{\beta} e^{-\frac{E_{aCKA}}{RT}} f_{CKA}(\alpha) \tag{S7}$$

where β is heating rate, K/min; α is the conversion rate at moment t;T is the temperature at moment t, K; T_0 is the temperature at $\alpha = 0$, K; A is pre-exponential factor; $f(\alpha)$ is the function versus conversion rate reflecting reaction mechanism; E_a is activation energy, J/mol; R is the ideal gas constant, 8.314 J/(mol·K);

(2) Thermodynamics

The pre-exponential factors (A_K) were calculated by Kissinger method using Eq.(S2). The activation enthalpy ($\Delta H^{\neq}$), activation entropy ($\Delta S^{\neq}$) and Gibbs free energy of activation ($\Delta G^{\neq}$) were calculated by Eqs.(S8~S10) [14].

$$\Delta H^{\neq} = E_{aK} - RT_{p0} \tag{S8}$$

$$\Delta S^{\neq} = R\ln\frac{A_K h}{kT_{p0}} + \frac{\Delta H^{\neq} - E_{aK}}{T_{p0}} \tag{S9}$$

$$\Delta G^{\neq} = \Delta H^{\neq} - T_{p0}\Delta S^{\neq} \tag{S10}$$

where $\Delta H^{\neq}$ is the activation enthalpy, J/mol; E_{aK} is the activation energy calculated by Kissinger method, J/mol; $\Delta S^{\neq}$ is the activation entropy, J/(mol·K); A_K is pre-exponential factor calculated by Kissinger method, s^{-1}; h is the Planck constant, 6.626×10^{-34} J/s; k is the Boltzmann constant, 1.3806×10^{-23} J/K; T_{p0} is the peak temperatures when the heating rate is zero, K; $\Delta G^{\neq}$ is the Gibbs free energy of activation, J/mol.

S4.2 DSC curves under different heating rates

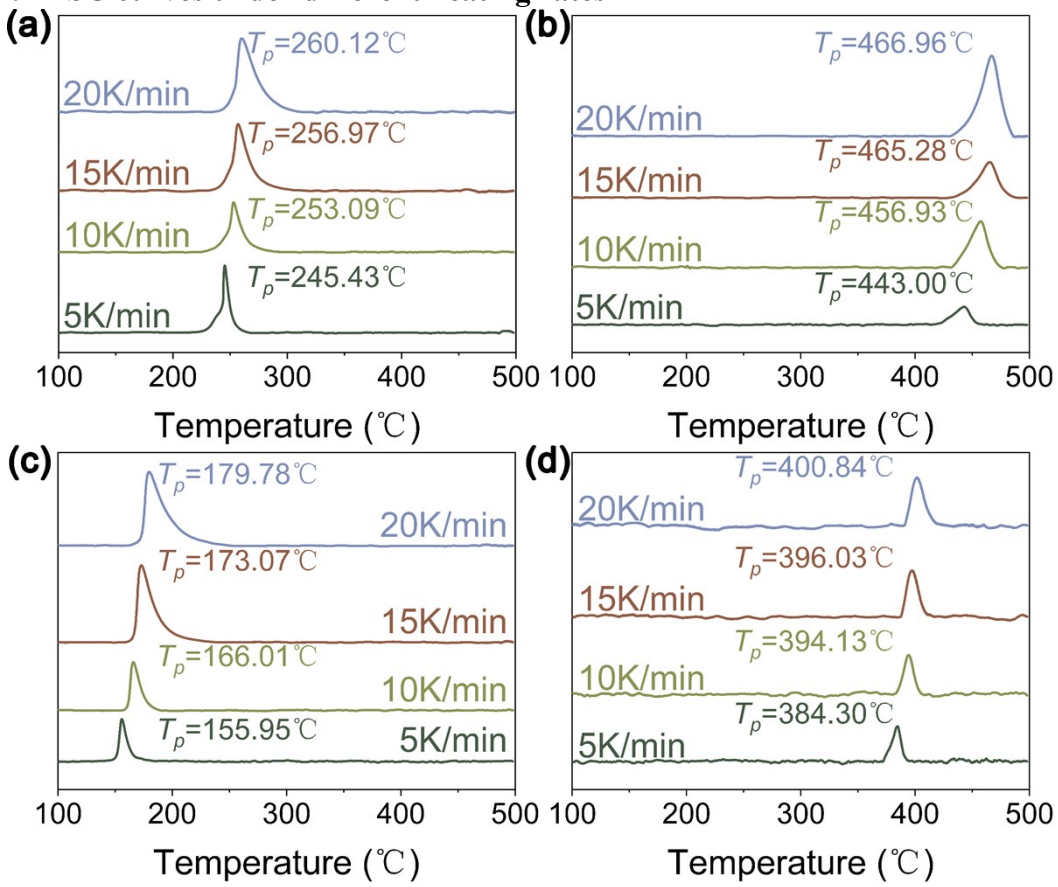

Fig. S2 The DSC curves of co-formers at different heating rates ((a) CL-20; (b) DATC; (c) DATF; (d) BTAAT)

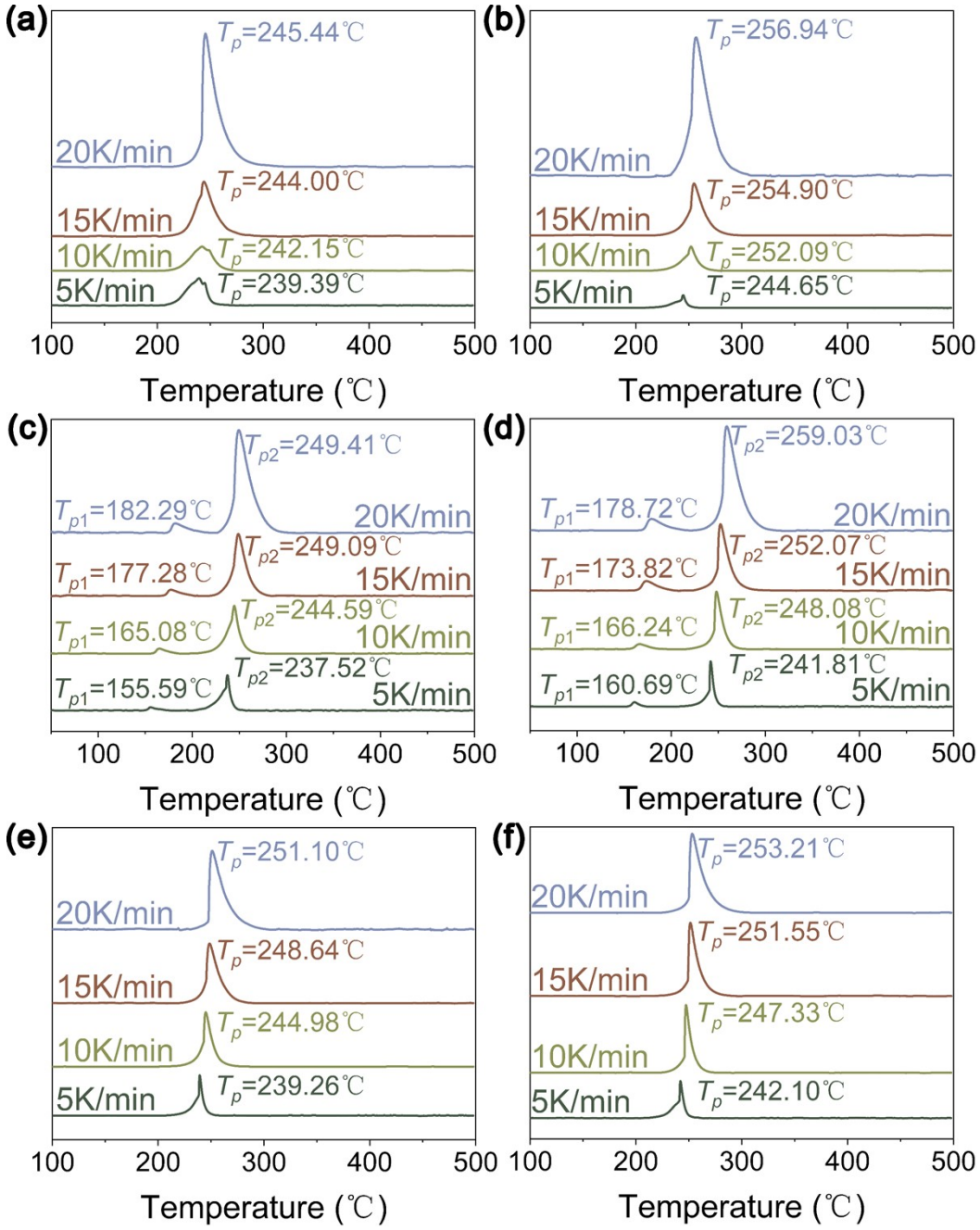

Fig. S3 The DSC curves of CACs and PMs at different heating rates ((a) 1-CAC; (b) 1-PM; (c) 2-CAC; (d) 2-PM; (e) 3-CAC; (f) 3-PM)

S4.3 Kinetics and thermodynamics

S4.3.1 Fitting results of DSC data by Kissinger and Ozawa methods

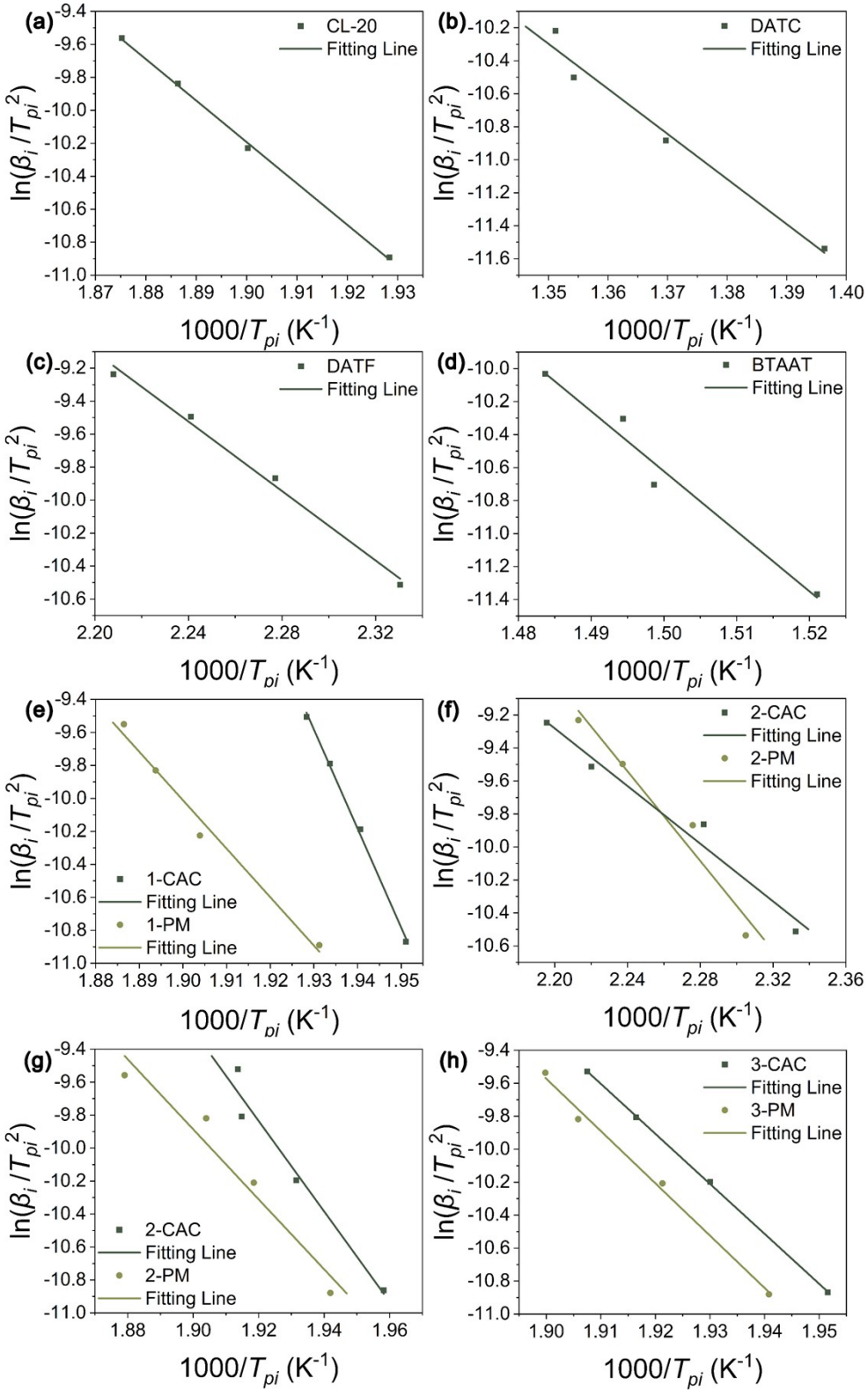

Fig. S4 The fitting lines of DSC data of co-formers, CACs and PMs based on Kissinger method ((a) CL-20; (b) DATC; (c) DATF; (d) BTAAT; (e) CL-20/DATC; (f) the first exothermic peak of CL-20/DATF; (g) the second exothermic peak of CL-20/DATF; (h) CL-20/BTAAT)

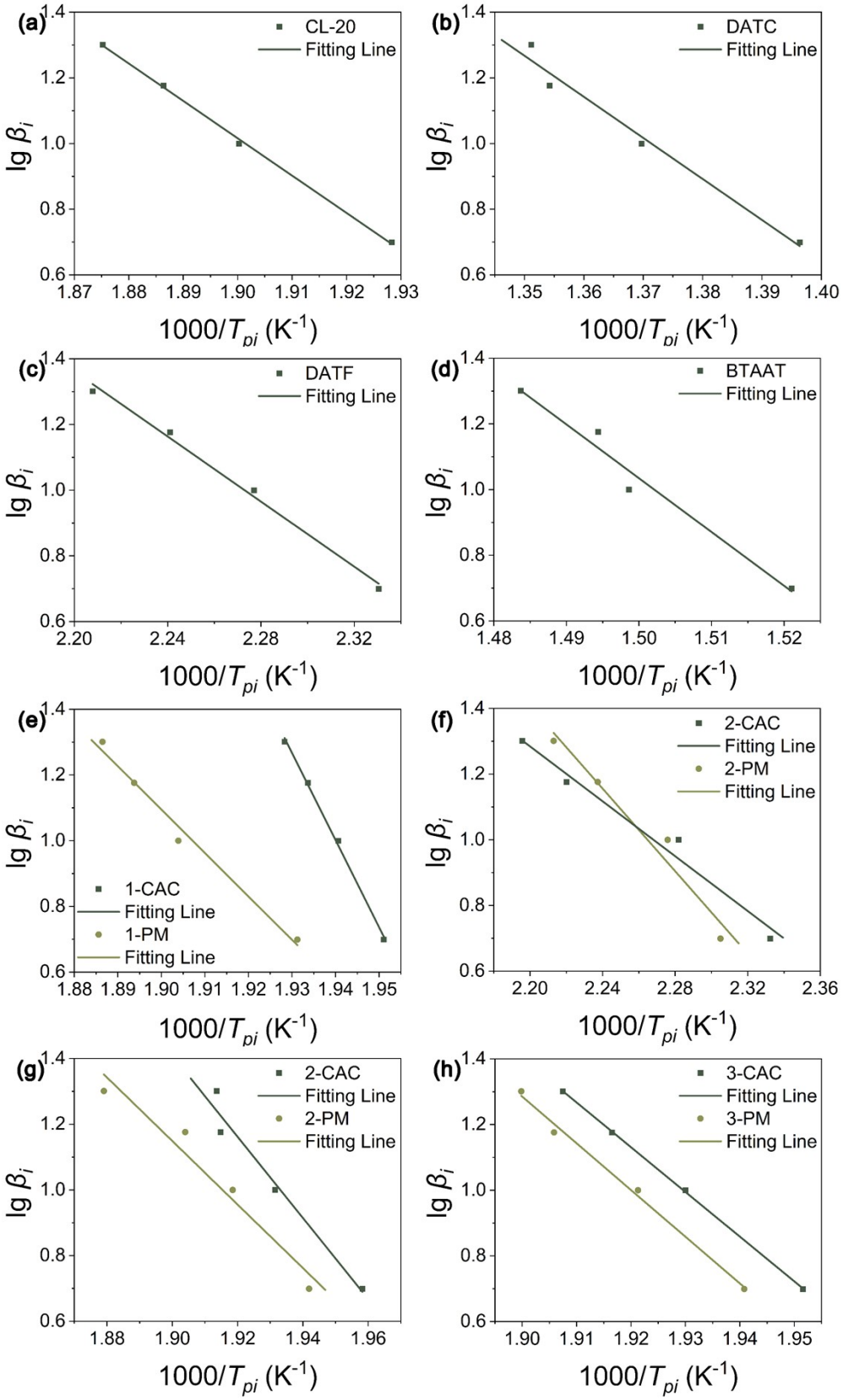

Fig. S5 The fitting lines of DSC data of co-formers, CACs and PMs based on Ozawa method ((a) CL-20; (b) DATC; (c) DATF; (d) BTAAT; (e) CL-20/DATC; (f) the first exothermic peak of CL-20/DATF; (g) the second exothermic peak of CL-20/DATF; (h) CL-20/BTAAT)

Table S4 The fitting equations, coefficients of determination (R^2), activation energy (E_a) and pre-exponential factor (A_K) of Kissinger and Ozawa methods of co-formers, CACs and PMs

Sample	Kissinger method				Ozawa method			Average values of E_a [kJ/mol]
	Fitting equation	R^2	E_{aK} [kJ/mol]	A_K [s^{-1}]	Fitting equation	R^2	E_{aO} [kJ/mol]	
CL-20	y=-25136.17193x+37.56663	0.9999	208.98	5.191×10^{20}	y=-11372.99964x+22.62487	0.9989	207.04	208.01
DATC	y=-27330.78754x+26.59948	0.9765	227.23	9.742×10^{15}	y=-12501.78624x+18.14473	0.9787	227.59	227.41
DATF	y=-10529.31699x+14.06190	0.9915	87.54	1.347×10^{10}	y=-4955.48214x+12.26376	0.9928	90.21	88.88
BTAAT	y=-36398.94983x+43.97618	0.9698	302.62	4.568×10^{23}	y=-16385.59465x+25.61306	0.9718	298.29	300.46
1-CAC	y=-60087.14890x+106.38607	0.9977	499.56	9.587×10^{50}	y=-26543.25697x+52.4959	0.9978	483.21	491.39
1-PM	y=-29378.51530x+45.80819	0.9847	244.25	2.303×10^{24}	y=-13213.69466x+26.20082	0.9857	240.55	242.40
2-CAC (first peak)	y=-8737.19601x+9.94086	0.9705	72.64	1.814×10^{8}	y=-4178.28911x+10.47662	0.9757	76.06	74.35
2-CAC (second peak)	y=-27432.29046x+42.83467	0.9651	228.07	1.099×10^{23}	y=-12362.39376x+24.89778	0.9675	225.05	226.56
2-PM (first peak)	y=-13585.50856x+20.89031	0.9568	112.95	1.606×10^{13}	y=-6284.64734x+15.23349	0.9619	114.41	113.68
2-PM (second peak)	y=-21227.95088x+30.44719	0.9476	176.49	3.548×10^{17}	y=-9673.89684x+19.52955	0.9523	176.11	176.30
3-CAC	y=-30322.12459x+48.31179	0.9998	252.10	2.906×10^{25}	y=-13618.76218x+27.27902	0.9998	247.92	250.01
3-PM	y=-31723.92573x+50.70302	0.9937	263.75	3.322×10^{26}	y=-14229.79581x+28.32183	0.9941	259.05	261.40

S4.3.2 Calculation of zero-heating-rate peak temperature, critical temperature of thermal explosion and thermodynamics parameters

Table S5 The values of T_{p0}, T_b and other coefficients of the formula for zero-heating-rate peak temperatures of co-formers, CACs and PMs

Sample	T_{p0} [K]	*b*	*c*×10²	*d*×10⁴	T_b [K]
CL-20	504.09	3.784	19.76	40.67	514.68
DATC	697.73	4.060	-6.800	-14.53	716.50
DATF	413.39	3.884	-16.60	35.33	430.75
BTAAT	628.85	8.320	-59.22	144.5	640.19
1-CAC	508.37	1.008	-3.820	6.667	512.82
1-PM	501.87	4.292	-24.70	51.47	510.82
2-CAC	431.86	-2.545	45.02	-132.0	455.01
	502.64	1.595	1.300	-21.47	512.27
2-PM	435.03	-1.226	22.90	-62.80	449.83
	501.16	3.863	-25.56	70.00	513.60
3-CAC	503.77	2.077	-7.560	11.47	512.50
3-PM	510.56	0.7807	4.180	-20.67	519.13

Table S6 The values of thermodynamics parameters of co-formers, CACs and PMs

Sample	$\Delta H^{\neq}$ [kJ/mol]	$\Delta S^{\neq}$ [J/(mol·K)]	$\Delta G^{\neq}$ [kJ/mol]
CL-20	204.79	138.98	134.73
DATC	221.43	45.79	189.48
DATF	84.10	-62.03	109.74
BTAAT	297.39	193.50	175.71
1-CAC	495.34	718.32	130.17
1-PM	240.08	208.83	135.27
2-CAC	69.05	-98.20	111.46
	223.89	183.52	131.64
2-PM	109.33	-3.56	110.88
	172.32	78.43	133.02
3-CAC	247.91	229.88	132.10
3-PM	259.51	250.02	131.86

S4.3.3 Analysis results of DSC data by Friedman method

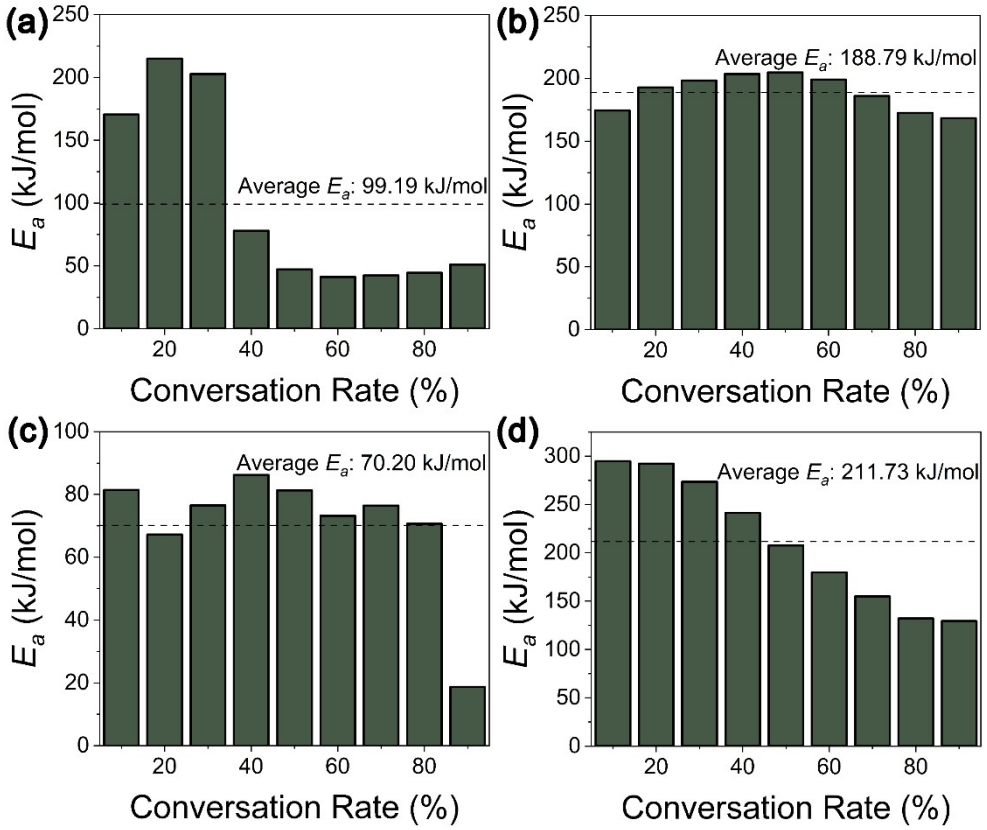

Fig. S6 The activation energies of (a) CL-20, (b) DATC, (c) DATF and (d) BTAAT based on Friedman method

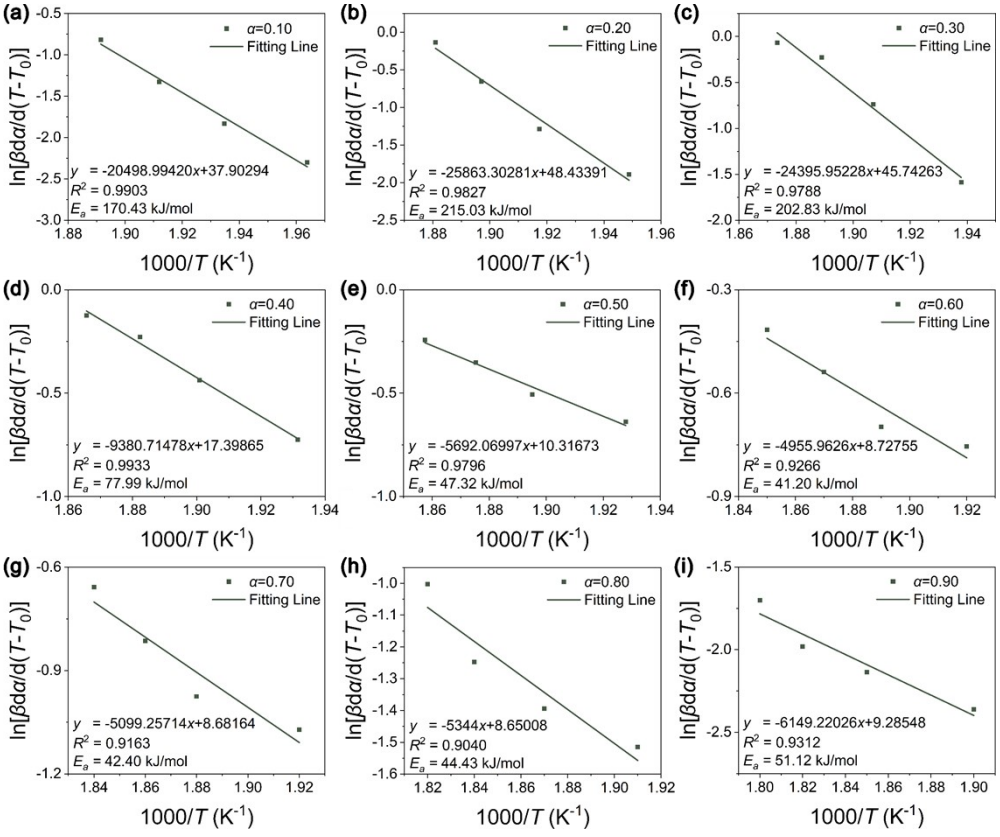

Fig. S7 The fitting lines of DSC data of CL-20 based on Friedman method

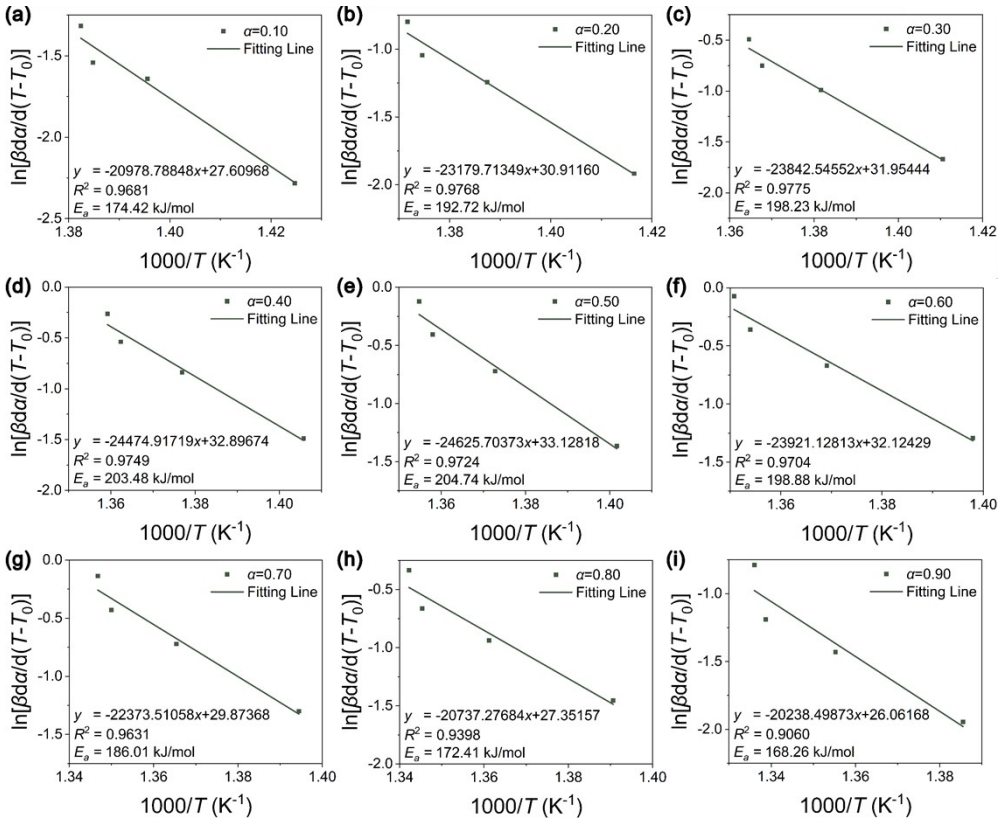

Fig. S8 The fitting lines of DSC data of DATC based on Friedman method

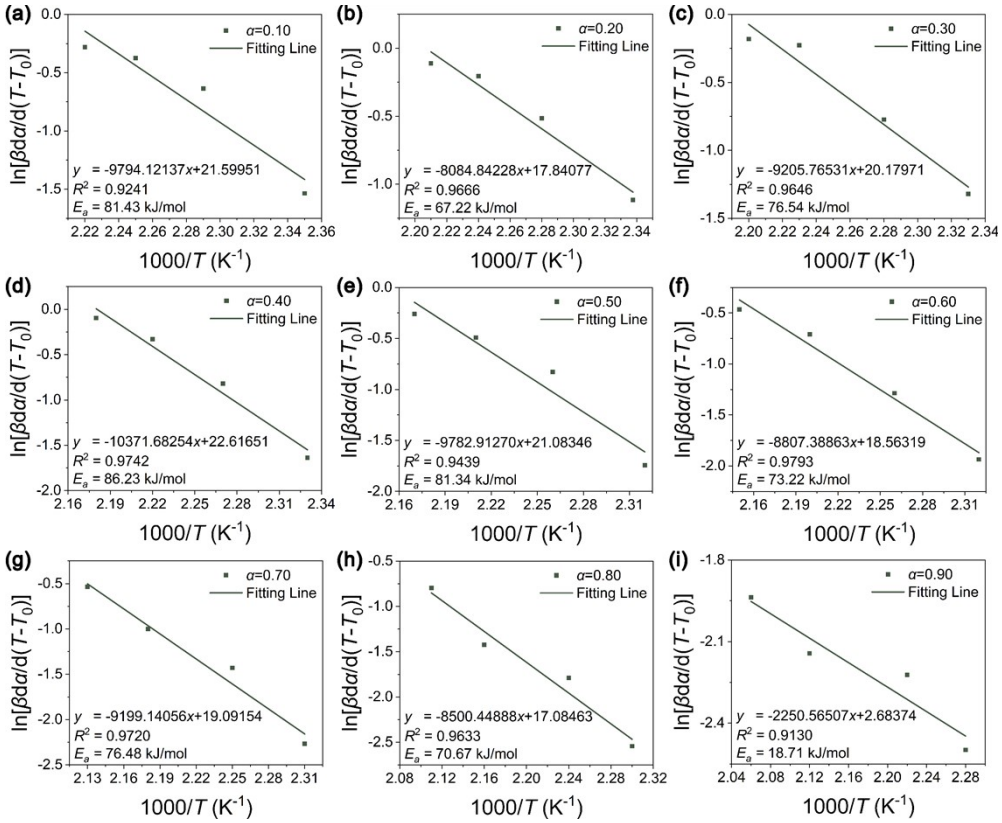

Fig. S9 The fitting lines of DSC data of DATF based on Friedman method

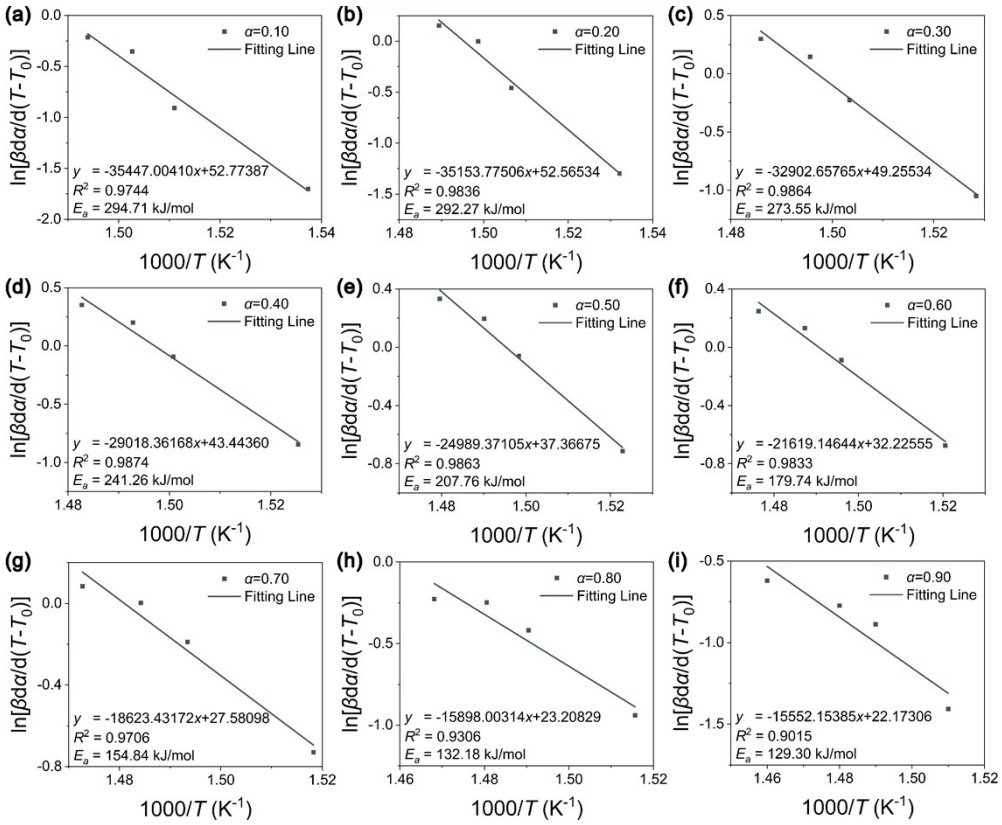

Fig. S10 The fitting lines of DSC data of BTAAT based on Friedman method

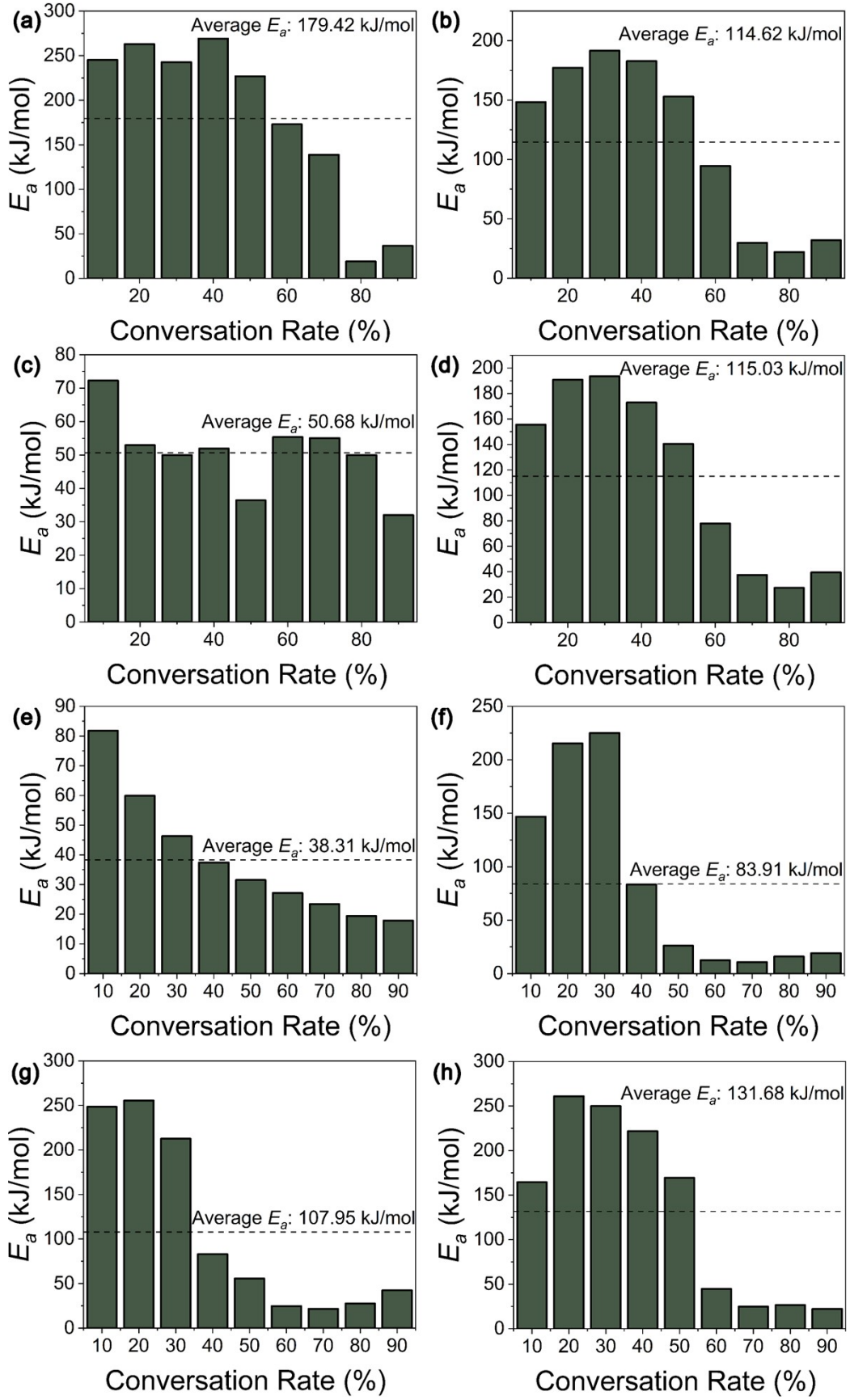

Fig. S11 The activation energies of (a) 1-CAC, (b) 1-PM, (c) 2-CAC (first peak), (d) 2-CAC (second peak), (e) 2-PM (first peak), (f) 2-PM (second peak), (g) 3-CAC and (f) 3-CAC based on Friedman method

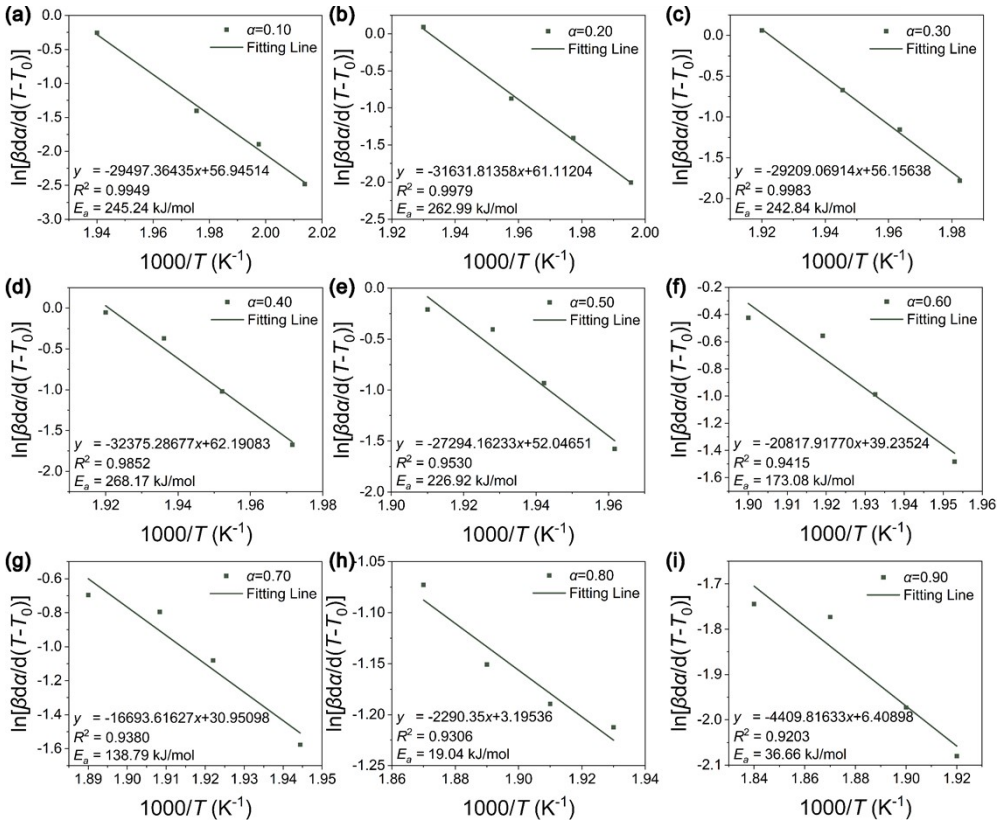

Fig. S12 The fitting lines of DSC data of 1-CAC based on Friedman method

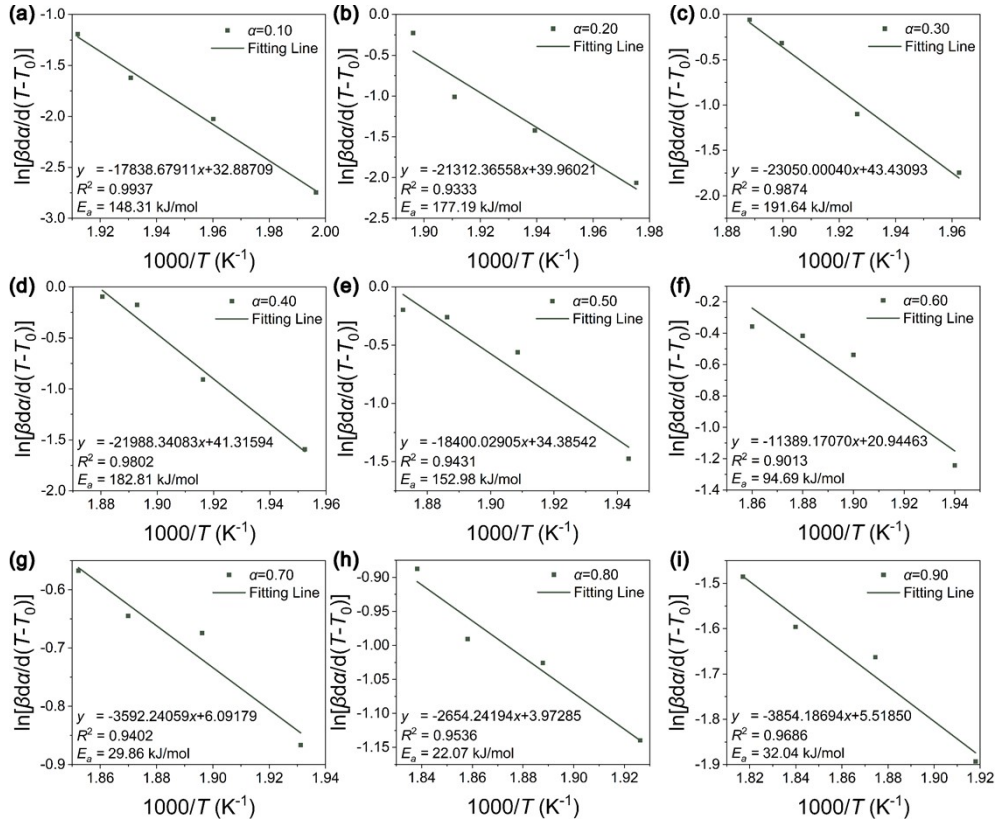

Fig. S13 The fitting lines of DSC data of 1-PM based on Friedman method

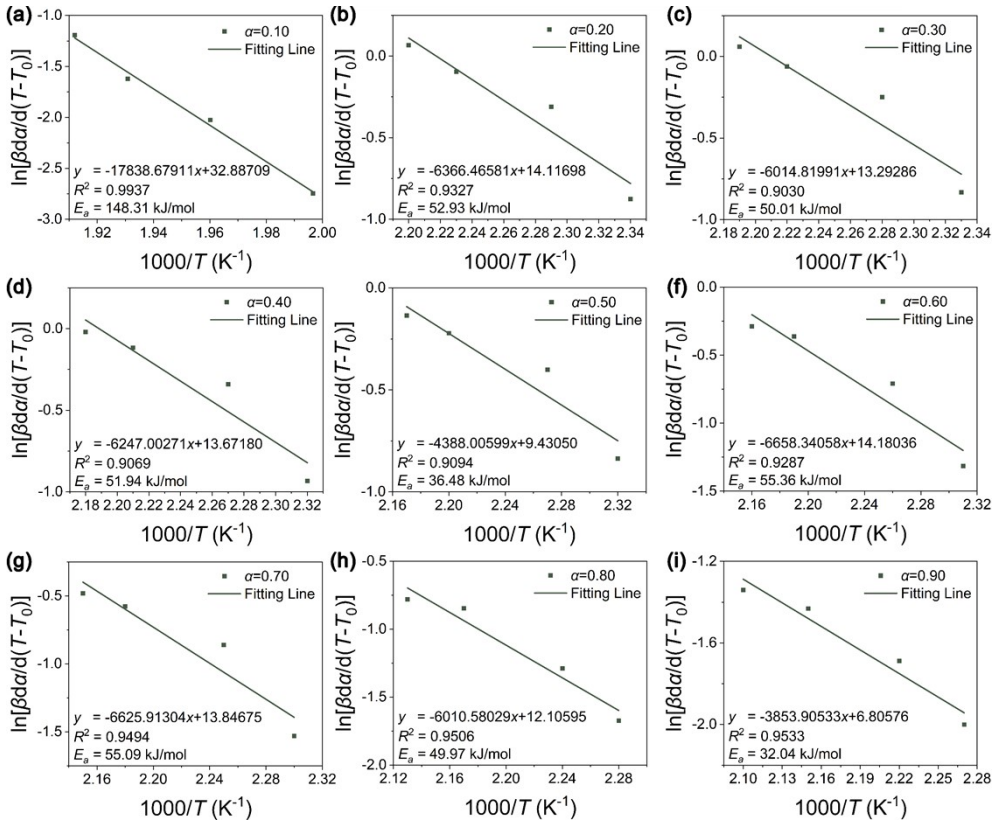

Fig. S14 The fitting lines of DSC data of 2-CAC (first exothermic peak) based on Friedman method

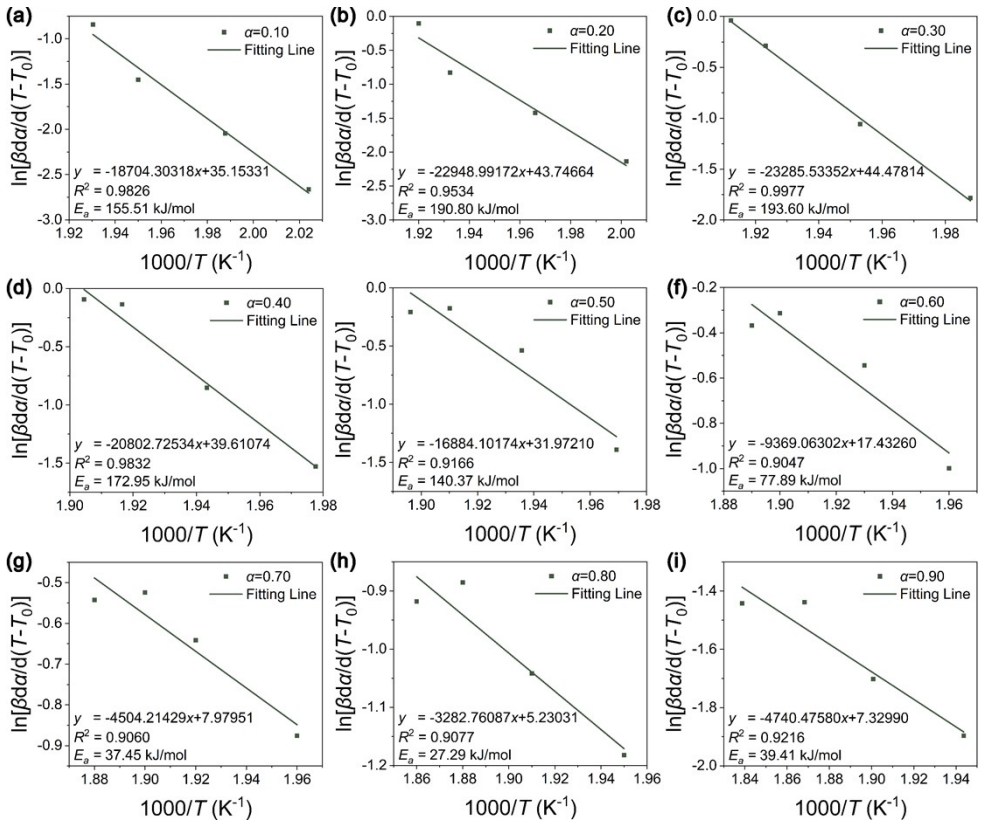

Fig. S15 The fitting lines of DSC data of 2-CAC (second exothermic peak) based on Friedman method

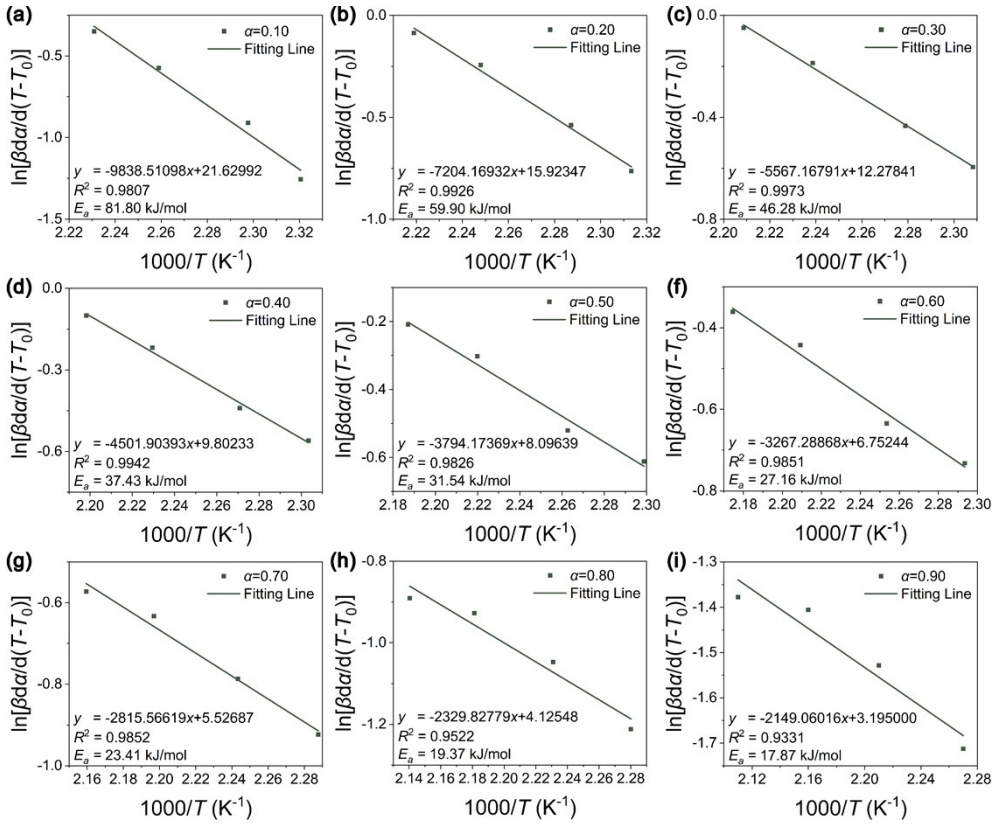

Fig. S16 The fitting lines of DSC data of 2-PM (first exothermic peak) based on Friedman method

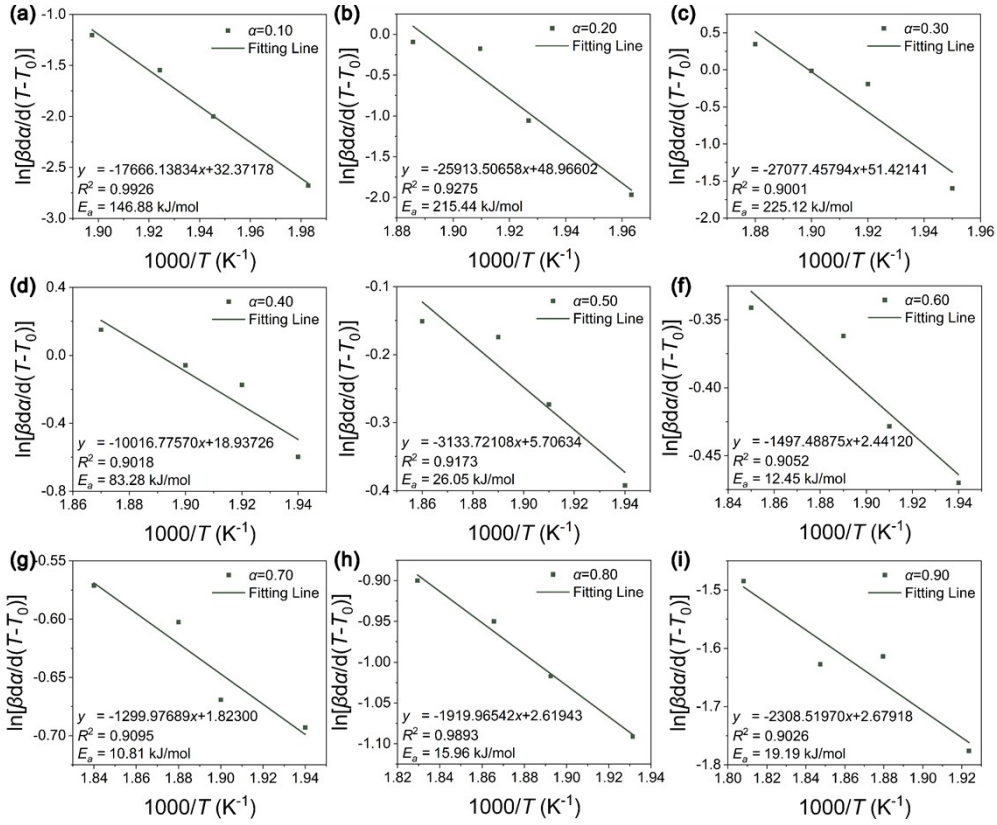

Fig. S17 The fitting lines of DSC data of 2-PM (second exothermic peak) based on Friedman method

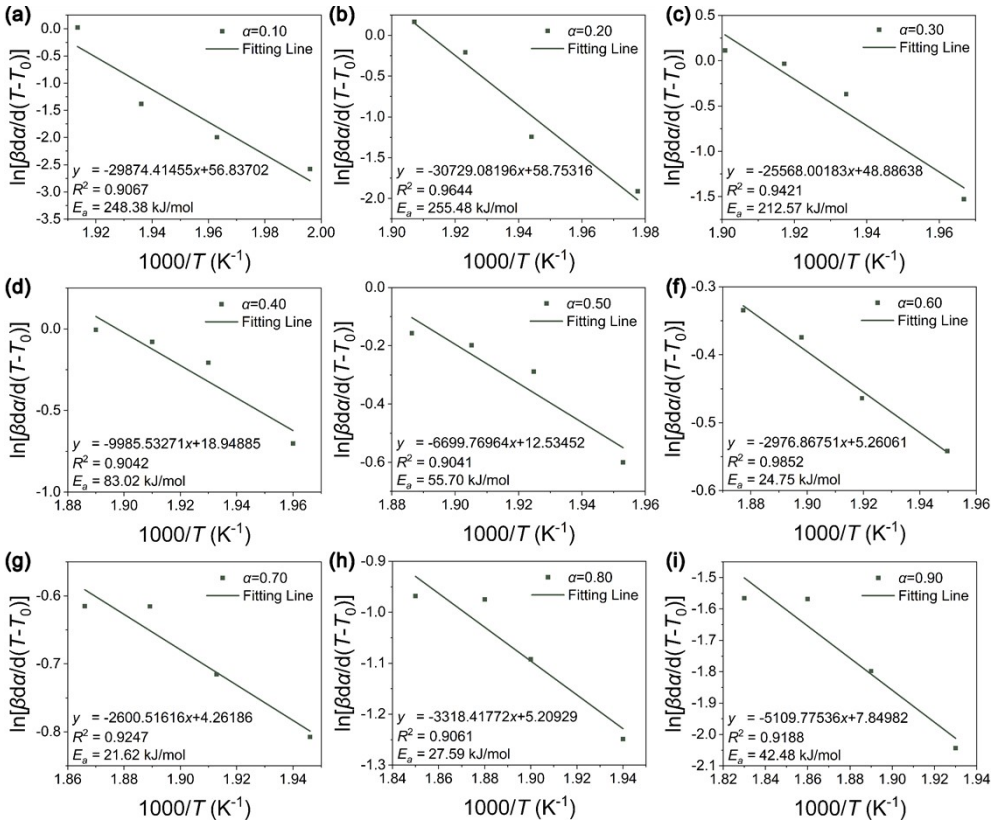

Fig. S18 The fitting lines of DSC data of 3-CAC based on Friedman method

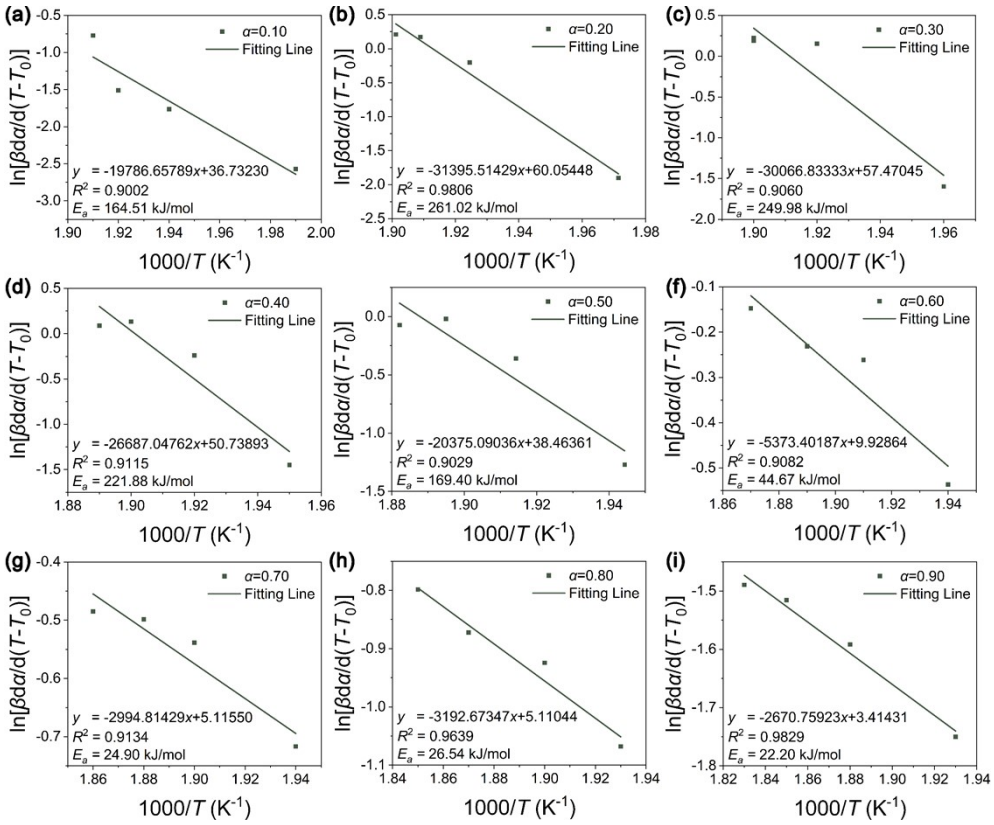

Fig. S19 The fitting lines of DSC data of 3-PM based on Friedman method

S4.3.4 Analysis results of DSC data by CKA method

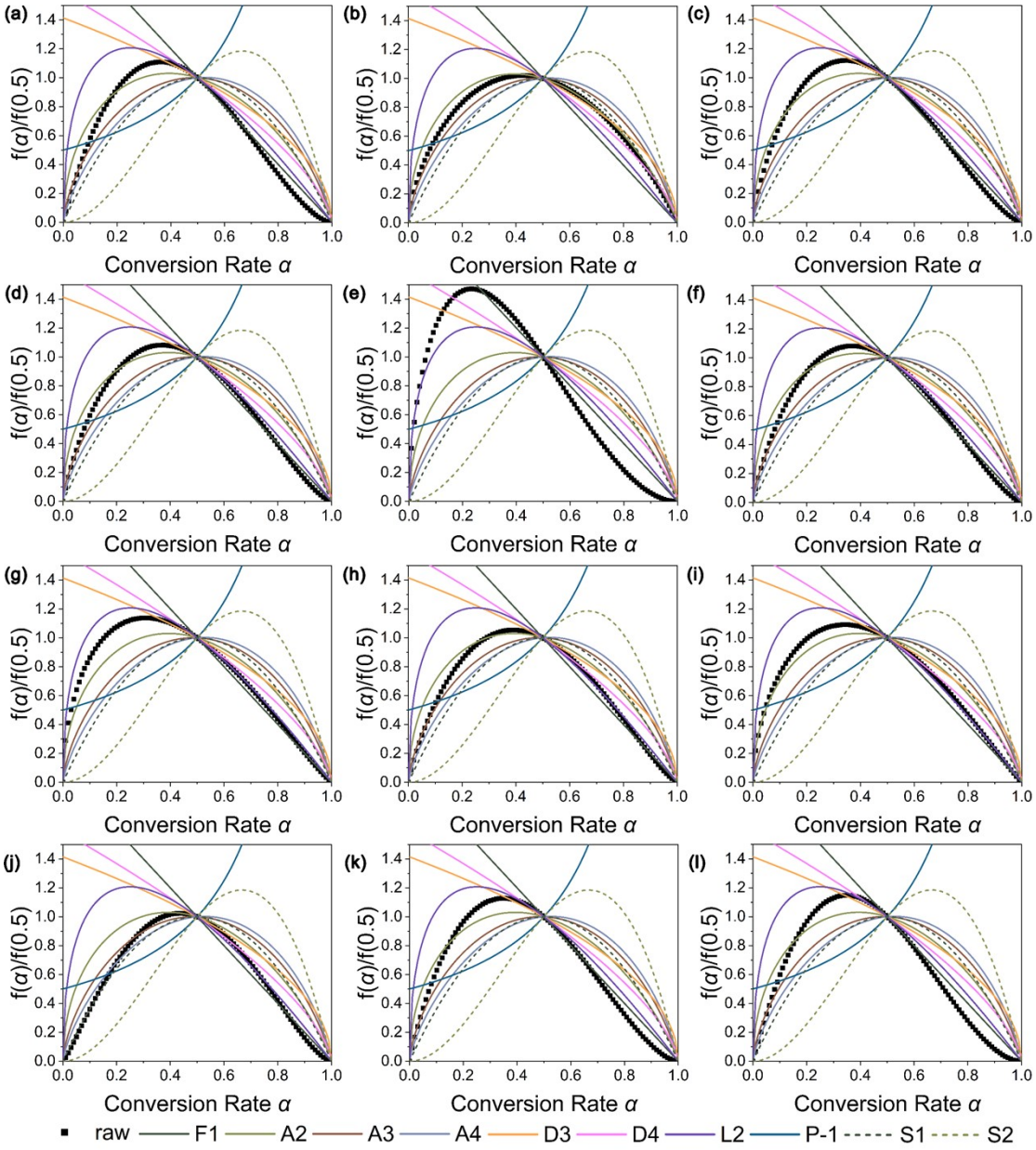

Fig. S20 The Analysis results of DSC data based on CKA method ((a) CL-20; (b) DATC; (c) DATF; (d) BTAAT; (e) 1-CAC; (f) 1-PM; (g) 2-CAC (first exothermic peak); (h) 2-CAC (second exothermic peak); (i) 2-PM (first exothermic peak); (j) 2-PM (second exothermic peak); (k) 3-CAC; (l) 3-PM)

S5 Theoretical calculation

S5.1 Calculation details

Geometry optimization and frequency analysis were performed on single molecules of CL-20 and NEMs. The bimolecular model of optimized CL-20 and NEMs were established using GaussView 6.0. Geometry optimization and frequency analysis were then performed on bimolecular model. Above calculations were conducted using Gaussian 16 (Rev. C.01)[15] under conditions: B3LYP[16, 17]/6-311G(d,p)[18] EM=GD3.[19]

Multiwfn Version 3.8(dev)[20, 21] was used for independent gradient model based on Hirshfeld partition (IGMH) analysis.[22] The result was then visualized using VMD Version 1.9.3.[23]

S5.2 Calculation results

The Cartesian coordinates of optimized CL-20/DATC, CL-20/DATF and CL-20/BTAAT were listed in Table S7-S9. The visualized calculation results were shown in Fig. S21.

Table S7 Cartesian coordinates of CL-20/DATC

C	-1.6499	1.93032	1.3781
H	-2.42058	1.16662	1.38451
C	-1.74414	2.89192	0.11783
N	-0.35314	1.30513	1.37866
N	-1.81489	2.82983	2.53113
H	-2.5649	2.63905	-0.54523
N	-0.5015	2.81891	-0.60534
N	-1.95192	4.22812	0.69855
C	0.79904	2.17229	1.37733
N	-0.21751	-0.06249	1.75004
C	-1.48623	4.18581	2.08631
N	-3.0151	2.68083	3.31989
C	0.705	3.13169	0.11991
N	-0.50012	2.82125	-2.02898
N	-3.22871	4.86018	0.46364
H	1.69695	1.5653	1.38414
N	0.802	3.14289	2.48763
O	-1.25101	-0.65499	1.9721
O	0.90996	-0.50206	1.75553
C	0.1031	4.35885	2.09947
H	-1.96923	4.93884	2.697
O	-3.31745	3.63303	4.00141
O	-3.55719	1.59943	3.26096
H	1.55232	3.04093	-0.54982
N	0.67306	4.45786	0.76418
O	-1.58983	2.80242	-2.55875
O	0.58731	2.79046	-2.55906
O	-3.83915	4.47621	-0.50933
O	-3.52466	5.74741	1.23033
N	0.66144	2.68999	3.80358
H	0.39003	5.19971	2.71956

N	0.37687	5.59167	0.00042
O	0.95808	1.52875	3.99936
O	0.28826	3.51826	4.61233
O	-0.0105	6.56301	0.62158
O	0.5693	5.49134	-1.19445
N	-0.29413	-5.33027	-4.7398
C	1.06621	-4.91633	-4.97217
N	1.69185	-4.06123	-4.15264
N	0.91476	-3.66746	-3.14169
C	-0.44637	-4.0816	-2.90917
N	-1.07159	-4.9366	-3.72874
N	-0.69045	-6.19417	-5.7082
C	0.44411	-6.27239	-6.49222
N	1.51235	-5.52439	-6.08484
N	1.31089	-2.80359	-2.17344
C	0.17621	-2.72531	-1.38961
N	-0.89203	-3.47343	-1.79654
N	0.47239	-7.04981	-7.59278
N	0.14781	-1.94762	-0.2893
H	1.31086	-7.08932	-8.1466
H	-0.33638	-7.58529	-7.85829
H	-0.69076	-1.90814	0.2644
H	0.9564	-1.41187	-0.02381

Table S8 Cartesian coordinates of CL-20/DATF

C	0.18082	0.84906	0
H	-0.24094	0.97194	-0.9921
C	1.76884	0.84903	0.00005
N	-0.2752	-0.39356	0.56604
N	-0.17977	1.99365	0.85188
H	2.19067	0.97192	-0.99202
N	2.22476	-0.39362	0.56609
N	2.12942	1.99361	0.85197
C	0.18253	-0.72307	1.89321
N	-1.40611	-1.05956	0.0145
C	0.9748	2.29595	1.70049
N	-0.82469	3.11648	0.21298
C	1.76695	-0.7231	1.89325
N	3.35591	-1.05947	0.01482
N	2.77439	3.11643	0.21308
H	-0.24374	-1.67538	2.18669
N	-0.11108	0.32344	2.88993
O	-1.87973	-0.55962	-0.9826
O	-1.74358	-2.08093	0.56889
C	0.97476	1.29078	2.94376
H	0.97481	3.32816	2.02886
O	-0.77102	4.16472	0.81372
O	-1.40054	2.8766	-0.8251
H	2.19318	-1.67542	2.18676
N	2.06057	0.32342	2.88994

O	3.82965	-0.55954	-0.98224
O	3.69337	-2.08078	0.56931
O	3.35029	2.87653	-0.82496
O	2.72074	4.16466	0.81384
N	-1.42132	0.79014	3.03842
H	0.97477	1.83964	3.87791
N	3.37084	0.79008	3.03835
O	-2.29747	0.04244	2.65355
O	-1.53947	1.87964	3.56607
O	3.48904	1.87964	3.56585
O	4.24692	0.04241	2.65328
C	5.97788	5.18544	-0.30654
C	6.10906	5.87298	0.95595
N	5.63211	6.06565	-1.19582
N	6.2315	3.86502	-0.59726
N	5.8331	7.12741	0.76848
N	6.4495	5.41757	2.22981
O	5.55284	7.25875	-0.53166
H	5.8871	3.58745	-1.507
H	6.00052	3.20803	0.13684
N	6.76055	4.21146	2.22264
N	7.10366	3.74495	3.4179
C	7.41368	2.40624	3.55092
H	7.02082	4.35009	4.23195
C	7.69737	1.44293	2.51844
N	7.53062	1.83551	4.70428
N	7.97308	0.3223	3.11024
N	7.62192	1.59904	1.1506
O	7.87135	0.55254	4.44671
H	8.04718	0.83101	0.64746
H	7.91731	2.50456	0.80686

Table S9 Cartesian coordinates of CL-20/BTAAT

C	-0.79401	-0.02818	-1.16051
H	-1.21577	0.09471	-2.15261
C	0.79402	-0.0282	-1.16046
N	-1.25002	-1.2708	-0.59448
N	-1.15459	1.11642	-0.30863
H	1.21585	0.09469	-2.15253
N	1.24994	-1.27086	-0.59442
N	1.15459	1.11638	-0.30855
C	-0.79229	-1.60031	0.7327
N	-2.38093	-1.9368	-1.14601
C	-0.00002	1.41872	0.53998
N	-1.79951	2.23924	-0.94753
C	0.79212	-1.60034	0.73273
N	2.38109	-1.93671	-1.14569
N	1.79957	2.23919	-0.94743
H	-1.21856	-2.55261	1.02618
N	-1.0859	-0.55379	1.72942

O	-2.85456	-1.43686	-2.14311
O	-2.7184	-2.95816	-0.59162
C	-0.00006	0.41355	1.78324
H	-0.00001	2.45093	0.86835
O	-1.74585	3.28748	-0.34679
O	-2.37537	1.99937	-1.98561
H	1.21836	-2.55265	1.02625
N	1.08575	-0.55382	1.72943
O	2.85483	-1.43678	-2.14275
O	2.71855	-2.95802	-0.5912
O	2.37547	1.9993	-1.98547
O	1.74592	3.28743	-0.34667
N	-2.39615	-0.0871	1.87791
H	-0.00005	0.9624	2.71739
N	2.39601	-0.08716	1.87784
O	-3.27229	-0.83479	1.49303
O	-2.51429	1.0024	2.40555
O	2.51422	1.00241	2.40534
O	3.2721	-0.83483	1.49277
N	-0.37457	-3.29822	-7.01873
C	0.15218	-3.63548	-5.7972
N	-0.53881	-4.22621	-4.79235
N	-1.84211	-4.5024	-5.01179
C	-2.35676	-4.16718	-6.21965
N	-1.65183	-3.5689	-7.2338
C	2.34495	-3.4956	-4.60823
N	1.48328	-3.31275	-5.67563
C	-4.67846	-4.98405	-5.79084
N	-3.67172	-4.40521	-6.54363
N	3.6515	-3.10144	-4.68428
N	4.31061	-3.3987	-3.47055
C	3.31175	-3.95744	-2.76275
N	2.088	-4.03848	-3.41873
N	-5.93846	-5.13373	-6.29902
N	-6.77101	-5.74717	-5.33649
C	-5.90992	-5.91185	-4.31554
N	-4.6154	-5.45922	-4.54751
N	3.45461	-4.42119	-1.49181
N	-6.24889	-6.47781	-3.12578
H	1.85369	-2.87841	-6.51131
H	-3.90089	-4.09791	-7.48026
H	4.16913	-2.6633	-5.42614
H	-6.32569	-4.88725	-7.1932
H	2.6609	-4.82578	-1.02881
H	4.34032	-4.36003	-1.02337
H	-5.54903	-6.56595	-2.41132
H	-7.18483	-6.80268	-2.96406

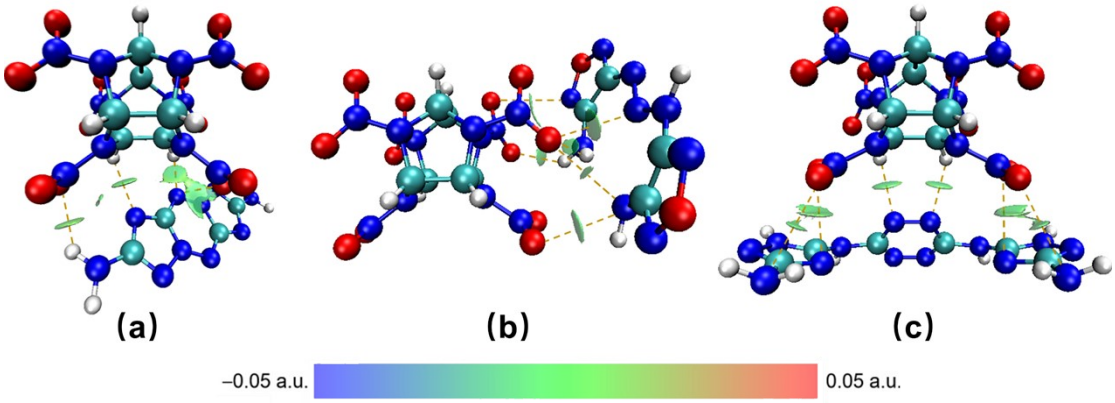

Fig. S21 Visualized results of intermolecular interactions of (a) CL-20/DATC, (b) CL-20/DATF and (c) CL-20/BTAAT

Reference

1. Y. F. Chang, North University of China, 2024.
2. G. F. Rudakov, V. P. Sinditskii, I. A. Andreeva, A. I. Botnikova, P. R. Veselkina, S. K. Kostanyan, N. V. Yudin, V. V. Serushkin, G. V. Cherkaev and O. V. Dorofeeva, *Chem. Eng. J.*, 2022, 450, 138073.
3. J. Zhu, Q. Chen, S. Jing, K. Li, Z. Wang, Y. Wang and J. Deng, *Heterocycles*, 2023, 106, 1866-1876.
4. A. Shlomovich, T. Pechersky, A. Cohen, Q. L. Yan, M. Kosa, N. Petrutik, N. Tal, A. Aizikovich and M. Gozin, *Dalton Trans.*, 2017, 46, 5994-6002.
5. B. Tan, J. Su, J. Zhang, C. Tang, J. Dou, X. Yang, M. Xu, S. Zeng, W. Li, J. Luan, G. Zhang, S. Song, Q. Zhang, X. Lu, B. Wang and N. Liu, *J. Mater. Chem. A*, 2025, 13, 25103-25109.
6. *Recommendations on the Transport of Dangerous Goods*, United Nations Publication, New York, 2019.
7. C.-j. Zuo and C.-y. Zhang, *Energ. Mater. Front.*, 2025, 6, 189-194.
8. X. Zhou, Z. Wang, H. Huang, Y. Liu, S. Li, W. Qian, S. Huang and J. Xu, *Nat. Commun.*, 2026, 17, 3271.
9. D.-K. Li, W.-S. Dong, H.-Z. Mei, M.-Q. Xu, Z.-J. Lu, Q.-Y. Yu and J.-G. Zhang, *Inorg. Chem. Commun.*, 2026, 184, 115941.
10. C. H. Hou, J. Y. Li, X. R. Jia, J. J. Ma, H. Z. Zhang and Y. H. Luo, *Fuel*, 2025, 391, 134801.
11. Z. T. Chen, Y. Wang, W. T. Ji, X. X. Guo, X. T. Liu, C. Y. Ma, J. J. Guo and Y. Su, *Organic Process Research & Development*, 2024, 28, 3674-3684.
12. J. Zhu, Q. X. Du, S. Y. Xu, X. W. Wu, F. Li and H. Qian, *J. Anal. Appl. Pyrolysis*, 2026, 196, 107700.
13. P. E. Sánchez-Jiménez, L. A. Pérez-Maqueda, A. Perejón and J. M. Criado, *Polymer Degradation and Stability*, 2010, 95, 733-739.
14. S. Bai, D. He, J. Zhao, L. Wang, L. Chen and J. Wang, *FirePhysChem*, 2025, DOI: 10.1016/j.fpc.2025.10.004.
15. M. J. Frisch, G. W. Trucks, H. B. Schlegel, G. E. Scuseria, M. A. Robb, J. R. Cheeseman, G. Scalmani, V. Barone, G. A. Petersson, H. Nakatsuji, X. Li, M. Caricato, A. V. Marenich, J. Bloino, B. G. Janesko, R. Gomperts, B. Mennucci, H. P. Hratchian, J. V. Ortiz, A. F. Izmaylov, J. L. Sonnenberg, Williams, F. Ding, F. Lipparini, F. Egidi, J. Goings, B. Peng, A. Petrone, T. Henderson, D. Ranasinghe, V. G. Zakrzewski, J. Gao, N. Rega, G. Zheng, W. Liang, M. Hada, M. Ehara, K. Toyota, R. Fukuda, J. Hasegawa, M. Ishida, T. Nakajima, Y. Honda, O. Kitao, H. Nakai, T. Vreven, K. Throssell, J. A. M. Jr., J. E. Peralta, F. Ogliaro, M. J. Bearpark, J. J. Heyd, E. N. Brothers, K. N. Kudin, V. N. Staroverov, T. A. Keith, R. Kobayashi, J. Normand, K. Raghavachari, A. P. Rendell, J. C. Burant, S. S. Iyengar, J. Tomasi, M. Cossi, J. M. Millam, M. Klene, C. Adamo, R. Cammi, J. W. Ochterski, R. L. Martin, K. Morokuma, O. Farkas, J. B. Foresman and D. J. Fox, 2016, Gaussian 16 Rev. C.01, Wallingford, CT.
16. A. D. Becke, *The Journal of Chemical Physics*, 1993, 98, 5648-5652.

17. C. T. Lee, W. T. Yang and R. G. Parr, *Physical Review B*, 1988, 37, 785-789.
18. R. Krishnan, J. S. Binkley, R. Seeger and J. A. Pople, *The Journal of Chemical Physics*, 1980, 72, 650-654.
19. S. Grimme, J. Antony, S. Ehrlich and H. Krieg, *Journal of Chemical Physics*, 2010, 132.
20. T. Lu and F. W. Chen, *Journal of Computational Chemistry*, 2012, 33, 580-592.
21. T. Lu, *Journal of Chemical Physics*, 2024, 161, 082503.
22. T. Lu and Q. X. Chen, *Journal of Computational Chemistry*, 2022, 43, 539-555.
23. W. Humphrey, A. Dalke and K. Schulten, *Journal of Molecular Graphics & Modelling*, 1996, 14, 33-38.